Matemática Contemporânea, Vol. 8, 269–295
http://doi.org/10.21711/231766361995/rmc813

FUNDAMENTAL SOLUTIONS OF A SYSTEM OF CONSERVATION LAWS WITH A SINGULAR CHARACTERISTIC FIELD

Dan Marchesin **Aparecido J. de Souza***

Abstract

We analyze the Riemann solution of a nonstrictly hyperbolic system of three conservation laws for Cauchy data in the neighborhood of a curve consisting of points where one of the characteristic line fields is linearly degenerate and has a saddle singularity. Even though the construction is nontrivial, the solution consists of sequences of shocks and rarefactions, with at most two intermediate constant states. Thus, this is an example where the Lax construction for Riemann solutions can be extended to hold even though some of its fundamental hypotheses are violated. The system describes three phase flow in porous media with four components employed in Petroleum Engineering. The line of singularities occurs in the contact field associated with the transport of the fourth component.

1. Introduction

We are interested in studying the behavior of the Riemann solution of a nonstrictly hyperbolic system of three conservation laws for states in a neighborhood of a curve where a characteristic line field is singular.

For strictly hyperbolic system possessing characteristic fields which are either genuinely nonlinear or linearly degenerate, there is a classical theorem due to Lax establishing existence and uniqueness of local Riemann solutions [8]. This result was generalized by Liu [7] for strictly hyperbolic systems which are

*This work was supported in part by the Conselho Nacional de Desenvolvimento Tecnológico e Científico under Grant CNPq/NSF 910087/92-0 and the Financiadora de Estudos e Projetos under Grant 65920311-00.

key words and phrases. linearly degenerate field, singular point, wave curve, bifurcation diagram, Riemann solution

allowed to lose genuine nonlinearity at isolated points of the rarefaction curves. Recently, the result was generalized again by Isaacson and Temple [5], for a class of non-strictly hyperbolic systems containing surfaces in state space where the characteristic speed corresponding to a linearly degenerate field coincides with the characteristic speed of a nondegenerate field.

In this work we consider an example of a non-strictly hyperbolic system of three equations containing coincidence surfaces (i.e., surfaces where two characteristic speeds coincide). However, the linearly degenerate field does not satisfy the main assumption in [5] that it has no singularities. The novel feature of this model is that there is a curve of points which are saddle singularities for the linearly degenerate field. The curve of singularities is also the set of states where branches of Hugoniot curves associated to contact discontinuities intersect each other. In this work, we characterize precisely the curve of singularities. In a future work we will show that similar curves exist and play analogous role in more general models.

Away from the curve of singularities the assumptions used in [5] are valid and there exist unique Riemann solutions [10]. Surprisingly, although on the curve of singularities the two main assumptions used in [5] fail, we find a unique solution consisting of at most three wave groups for the Riemann problem with initial data in a neighborhood of this curve. Thus this work is a step towards generalizing Lax's construction to systems where some of its main assumptions are violated. It also indicates that the right construct in this generalization is not the wave curve - a one-parameter family of wave groups - but rather wave surfaces - multiparameter families of sequences of wave groups.

The paper is divided in more six sections. In §2 we present the system we study. The system captures some essential mathematical features of multiphase fluid flow in porous media where mass is transfered between phases, which occurs in petroleum reservoirs. In §3, we establish some basic definitions about Riemann problems and about nonlinear waves. In §4, using explicit calculations, we determine and characterize the curve of singularities of the linearly degenerate field. Next, in §5, we review the contact entropy condition used in

the wave curve construction. In §6, we present the qualitative behavior of the Hugoniot curves and discuss the admissibility of the elementary waves which occur in the Riemann solution. Finally in §7, we construct the Riemann solution for initial states in a neighborhood of the curve of singularities.

2. The model

Let us consider the system of three conservation laws introduced in [10]:

$$\begin{array}{lcl} u_t & + & f(u,v,c)_x = 0 \\ v_t & + & g(u,v,c)_x = 0 \\ (cu)_t & + & (cf(u,v,c))_x = 0, \end{array} \tag{2.1}$$

where $f(u,v,c) = u^2/\{a(c)\, D(u,v,c)\}$, $g(u,v,c) = v^2/D(u,v,c)$ and $D(u,v,c) = u^2/a(c) + v^2 + (1-u-v)^2$. The dependent variables take values in the prism $\Omega = \{(u,v,c) \in I\!R^3 \,|\, 0 \leq u, v, u+v \leq 1 \text{ and } 0 \leq c << 1\}$, and $a(c)$ is a prescribed smooth function with $a(c) > 0$ and $\frac{da(c)}{dc} > 0$. The explicit calculations occurring in this work were performed utilizing the simplistic function $a(c) = 1 + c$. In the context of flow in porous media, u, v, $1-u-v$ may be thought of as the saturations of each of the three phases, water, oil and gas. The concentration of a polymer transported in the water phase is c; the presence of the polymer affects the viscosity of the water phase $a(c)$. The viscosities of the phases described by v, and $1-u-v$ are considered identically 1. With this interpretation, this is a model for polymer injection, a method used in Petroleum Engineering to improve oil recovery in reservoirs.

3. The Riemann problem

In this section we establish the definition of the Riemann problem for system (2.1) and we recall a few definitions about nonlinear waves.

First of all, the system (2.1) can be written in a compact notation as:

$$\begin{array}{c} \mathcal{H}(U)_t + \mathcal{F}(U)_x = 0\,, \quad x \in I\!R, \quad t \in I\!R^+, \quad \text{where} \\ U(x,t) = (u,v,c), \quad \mathcal{H}(U) = (u,v,cu), \quad \mathcal{F}(U) = (f(U), g(U), cf(U))\,. \end{array} \tag{3.1}$$

The *Riemann problem* for (3.1) is the initial value problem with piecewise constant initial data given by:

$$U(x,t=0) = \begin{cases} U_L, & \text{for} \quad x < 0 \\ U_R, & \text{for} \quad x > 0 \end{cases} \tag{3.2}$$

For differentiable solutions U with values in Ω, the system (3.1) can be written as:

$$U_t + A(U) \cdot U_x = 0 \quad ,$$

where $A(U)$ is the Jacobian matrix:

$$A = (D\mathcal{H})^{-1} D\mathcal{F} = \begin{pmatrix} f_u & f_v & f_c \\ g_u & g_v & g_c \\ 0 & 0 & f/u \end{pmatrix}. \tag{3.3}$$

A *rarefaction wave* connecting U_- to U_+ is a continuous piecewise smooth solution of system (3.1) depending on x/t, with initial data $U_L = U_-$ and $U_R = U_+$, given by:

$$U(x,t) = \begin{cases} U_-, & \text{if} \quad x/t \leq \lambda(U_-) \\ \psi(x/t), & \text{if} \quad \lambda(U_-) \leq x/t \leq \lambda(U_+), \text{ with } \lambda(\psi(x/t)) = x/t \,, \\ U_+, & \text{if} \quad x/t \geq \lambda(U_+) \,, \end{cases} \tag{3.4}$$

where $\lambda(U)$ is one of the characteristic speed of the matrix A in (3.3). The values of the function $\psi(x/t)$ in (3.4) must lie on a section of the integral curve through U_- of the characteristic line field; along this section the corresponding characteristic speed is monotonically increasing. Such maximal section of the integral curve is called a *rarefaction curve* through U_-. Isolated critical points of $\lambda(U)$ along the integral curve are called *inflection points.* The set of inflection points in state space is called a *inflection locus.* A characteristic field of A associated to $\lambda(U)$ is called *linearly degenerate* if $\lambda(U)$ is constant along its corresponding integral curves.

A *shock wave* connecting U_- to U_+ is a discontinuous (weak) solution of system (3.1), with initial data $U_L = U_-$ and $U_R = U_+$, given by:

$$U(x,t) = \begin{cases} U_-, \text{ if } x/t < \sigma \\ U_+, \text{ if } x/t > \sigma \,, \end{cases} \tag{3.5}$$

where σ is a real constant, called the *speed* of the shock between U_- and U_+. It is well know that a shock wave connecting U_- to U_+ must satisfy the Rankine-Hugoniot condition

$$\sigma[\mathcal{H}(U_+) - \mathcal{H}(U_-)] = [\mathcal{F}(U_+) - \mathcal{F}(U_-)]\,. \tag{3.6}$$

The *Hugoniot curve* $H(U_-)$ of U_- is the set of states U_+ satisfying (3.6), for σ varying on $\mathbb{R}$. For system (2.1), in general a Hugoniot curve consists of three branches emanating from U_- in the direction of the eigenvectors of A, [8], together with one or two detached branches [10]. We call a *secondary bifurcation point* of a Hugoniot curve $H(U_-)$ a state U^* distinct from U_- where two branches of $H(U_-)$ intersect each other. The *secondary bifurcation locus* is the set of states U_- for which $H(U_-)$ has a secondary bifurcation point U^*, [3].

If in (3.5) we have $\sigma = \lambda(U_-) = \lambda(U_+)$, the shock wave is called a *contact discontinuity.* A Hugoniot branch along which the shock speed σ is constant and coincides with a characteristic speed λ is called a *contact Hugoniot branch.*

According to [11], contact Hugoniot branches coincide with integral curves of linearly degenerate characteristic fields. Thus, we use the nomenclature *contact curves* for both.

A *composite wave* connecting U_- to U_+ consists of a rarefaction (or shock) wave connecting U_- to an intermediate state U_i, followed by a shock (or rarefaction) wave connecting U_i to U_+, with the shock speed coinciding with the characteristic speed at U_i.

A *wave group* connecting U_- to U is a sequence of rarefaction and shock waves with increasing wave speed and no embedded sector of constant states separating U_- from U.

A *forward (backward) wave curve* through U_- (U_+) is the locus of states U_+ (U_-) in state space Ω, such that the state U_- can be connected to U_+ by a single wave group.

A *Riemann solution* of system (3.1) with initial data U_L and U_R, given in (3.2), is a sequence of wave groups separated by sectors of constant states.

4. The Linearly Degenerate Field

In this section we characterize the linearly degenerate characteristic field of system (3.1) and a certain curve where this field is singular.

It is clear that one of the eigenvalues of matrix A in (3.3) is $\lambda^c = f/u$. The other characteristic speeds λ^s and λ^f are the eigenvalues of the 2×2 top left block of A associated with the subsystem (4.1) for $c = constant$:

$$\begin{aligned} u_t + f(u, v; c)_x &= 0 \\ v_t + g(u, v; c)_x &= 0 \,. \end{aligned} \tag{4.1}$$

Since we have $\lambda^s \leq \lambda^f$ in Ω, we use the superscripts s and f to indicate the *slow* and the *fast* waves of system (4.1), respectively. The Riemann problem for the subsystem (4.1) was studied in detail in [9]. The next theorem can be found in [10] as Proposition 3.1.

Theorem 4.1: *The field $e^c(U)$ of eigenvectors of A associated to $\lambda^c(U)$ is linearly degenerate, i.e., $\nabla\lambda^c(U) \cdot e^c(U) \equiv 0$.*

Let us denote e^c by X. From (3.3), the line field $X(U)$ turns out to be:

$$X = ((\lambda^c - g_v)f_c + f_v g_c, (\lambda^c - f_u)g_c + g_u f_c, (f_u - \lambda^c)(g_v - \lambda^c) - f_v g_u). \tag{4.2}$$

We are interested in studying the line field X. To do so, we establish the following:

Proposition 4.2: *The line field X has a curve of singularities interior to the domain Ω.*

Proof. A direct calculation using the formulas in Section 2, was performed using the *Mathematica* symbolic manipulation package. Eliminating denomina-

tors, the line field (4.2) can be written as $X = (X_1, X_2, X_3)$, where:

$$\begin{aligned} X_1(u,v,c) &= -\tfrac{u^2}{a(c)^3}\,(u - 2u^2 + u^3 - 2a(c)v - 2uv + 4a(c)uv \\ &\quad +2u^2v - 2a(c)u^2v + 2a(c)v^2 + 2uv^2 - 2a(c)uv^2)\,; \\ X_2(u,v,c) &= \tfrac{u^2v^2}{a(c)^3}\,(-2a(c) + u + 2a(c)u + 2a(c)v)\,; \\ X_3(u,v,c) &= \tfrac{u^2}{a(c)^3}\,(-a(c)u + u^3 + a(c)u^3 + 2a(c)^2v + 2a(c)uv \\ &\quad -2a(c)u^2v - 2a(c)^2u^2v - 2a(c)^2v^2 - 2a(c)uv^2 \\ &\quad -2a(c)^2uv^2)\,. \end{aligned} \tag{4.3}$$

A straightforward calculation shows that line field X vanishes at an interior curve α with $\frac{\partial \alpha}{\partial c} \neq 0$. This curve may be parametrized by c as:

$$\alpha(c) = (\frac{a(c)}{1 + a(c)}, \quad \frac{1}{2(1 + a(c))}, \quad c). \tag{4.4}$$

There exist two disjoint surfaces where coincidence of λ^c with λ^s and of λ^c with λ^f occurs. (See [10]). We denote these coincidence surfaces T^s and T^f, respectively. These surfaces subdivide the domain Ω in three distinct subregions: R_1 in which $\lambda^c < \lambda^s \leq \lambda^f$, R_2 in which $\lambda^s < \lambda^c < \lambda^f$ and R_3 in which $\lambda^s < \lambda^f < \lambda^c$. As shown in [5], if an integral curve of X crosses a coincidence surface at a state $U_0 = (u_0, v_0, c_0)$ away from curve α, then $X(U_0)$ is tangent to the plane $c = c_0$; also, such integral curve crosses planes $c = c_1 < c_0$ exactly twice. A special projection of typical contact curves for our model is exhibited in **Fig.** 4.1. Even though the three characteristic speeds are out of order, we maintain the nomenclature *slow* and *fast* for the two waves of system (4.1).

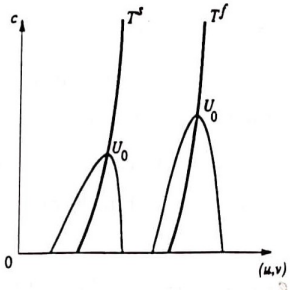

Fig. 4.1: Projection of two contact curves and the two coincidence surfaces.

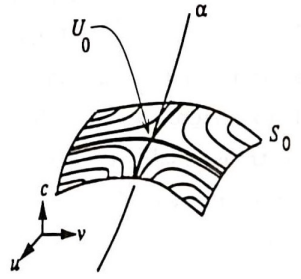

Fig. 4.2: The curve of singularities α and the line field X on S_0.

Let us study the degenerate characteristic field X near the curve of singularities α. Let $U_0 = (u_0, v_0, c_0)$ be an arbitrary state on α and consider the line field in a neighborhood of U_0. Since λ^c is constant along the integral curves of X, such integral curves lie on level surfaces of λ^c. In other words, the level surfaces are foliated by the integral curves of X. It is also easy to show that α is transversal to such level surfaces.

Now consider the level surface $S_0 = \{(u, v, c) \in \Omega \,|\, \lambda^c(U) = \lambda^c(U_0)\}$. A direct calculation shows that the plane π_0 tangent to the surface S_0 at the point U_0 is given by:

$$(c - c_0) = K(u - u_0), \tag{4.5}$$

where $K = (1 + a_0)$ and $a_0 = a(c_0)$.

Since we focus our attention to a neighborhood of U_0, let us consider the line field X restricted to π_0. Consider the basis $\{\mathbf{f}_1, \mathbf{f}_2\}$ spanning the plane π_0, with $\mathbf{f}_1 = \mathbf{e}_1 + K\mathbf{e}_3$ and $\mathbf{f}_2 = \mathbf{e}_2$, where $\{\mathbf{e}_i\}_{i=1}^3$ is the standard basis for $\mathbb{R}^3$. Substituting (4.5) in (4.3), the line field X can be written (for $p = (u, v, c_0 + K(u - u_0))$ on π_0) as

$$X = X_1(p)\,\mathbf{f}_1 + X_2(p)\,\mathbf{f}_2 + (X_3(p) - KX_1(p))\,\mathbf{e}_3. \tag{4.6}$$

Notice that the coefficients of $\mathbf{f}_1$ and $\mathbf{f}_2$ vanish at (u_0, v_0, c_0) while the coefficient of $\mathbf{e}_3$ vanishes quadratically at this point. Let $\tilde{X} = X_1\mathbf{f}_1 + X_2\mathbf{f}_2$ be the projection of X onto π_0 along $\mathbf{e}_3$. Linearizing $\tilde{X}$ near U_0 we obtain that the corresponding 2×2 Jacobian at U_0 is

$$det[\frac{\partial(X_1, X_2)}{\partial(u, v)}] = \frac{-1}{4(1 + a_0)^8} < 0. \tag{4.7}$$

This means that for any value c_0 the state U_0 on the singular curve α corresponds to a saddle point of the line field $\tilde{X}$ defined on the tangent plane π_0. Since α is transversal to horizontal planes $c = constant$, varying U_0 along α, we see that the line field X can be topologically visualized as a family of saddles centered on the curve α. See **Fig.** 4.2.

Now let us determine the invariant manifolds associated to the saddles at the curve of singularities α. To do so, as we saw in §3, we regard the contact

curves as Hugoniot contact branches. The next proposition and its Corollary can be found in [10].

Proposition 4.3: *For any fixed U_- in Ω, the Hugoniot curve of system (3.1) through U_- consists of two parts. The first one is the Hugoniot curve of system (4.1) lying on the plane $c = c_-$. The second one consists of contact branches with associated shock speed $\lambda^c(U_-)$.*

Corollary: *Let U_+ be a state of $H(U_-)$, with $u_- \neq u_+$, and associated shock speed σ. Then $\sigma < \lambda^c(U_-)$ if, and only if, $\sigma < \lambda^c(U_+)$ and $\sigma = \lambda^c(U_-)$ if, and only if, $\sigma = \lambda^c(U_+)$.*

One peculiarity of the Hugoniot curves in this model is that they may possess a detached contact branch in addition to the local contact branch through U_-. A typical Hugoniot curve for system (3.1) is exhibited in **Fig.** 4.3 in the three-dimensional state space $\{(u, v, c)\}$.

We obtain the invariant manifolds for the line of singularities α as surfaces generated by contact Hugoniot branches of $H(U_0)$, with U_0 varying along α. Actually, the same kind of calculations used to obtain the parametrization of α in (4.4) also characterize α as the set of states U^* where contact Hugoniot branches undergo a secondary bifurcation.

Thus, let U_0 be a state on α. Using equations (3.6) and the formula for λ^c, the contact Hugoniot branches of $H(U_0)$ are given by the following pair of equations:

$$\begin{aligned} \lambda^c(U) &= \lambda^c(U_0) \\ \lambda^c(U_0)(v - v_0) &= g(U) - g(U_0)\,. \end{aligned} \tag{4.8}$$

Using the parametrization (4.4) of α and substituting the coordinates of U_0

in (4.7), we obtain the following pair of equations, where $a = a(c)$:

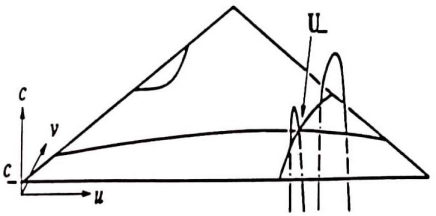

Fig. 4.3: Typical Hugoniot curve in state space Ω.

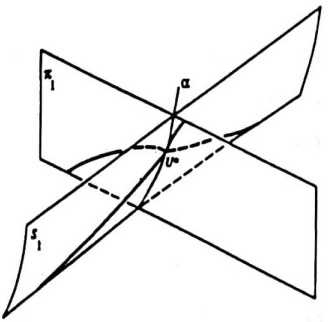

Fig. 4.4: Contact curves in the invariant manifolds of α.

$$\begin{aligned} 4(1+a_0)(uv-av^2)-u &= 0 \\ 2(1+a_0)(u-u^2-2av^2-2auv-au^2+2au+2av-a)-u &= 0\,. \end{aligned} \tag{4.9}$$

Near U_0 we have $uv - av^2 \neq 0$. Eliminating $1 + a_0$ from equations (4.8), we see that the two contact branches of $H(U_0)$ emanating from U_0 lie on the surfaces given by

$$(1-u-2v)(u+au-a) = 0.$$

Therefore the invariant manifolds are the plane π_1 with equation $1-u-2v = 0$ and the ruled surface S_1 given by $u + a(c)u - a(c) = 0$. We recall that the invariant manifolds are also the secondary bifurcation locus associated to the contact branches, which means that for U_- on π_1 or on S_1, the contact Hugoniot branches of $H(U_-)$ intersect each other precisely at a state U^* on α. The curve of singularities α and its invariant manifolds are represented in **Fig.** 4.4. In this figure two contact curves (Hugoniot branches) with the same characteristic speed lying on the invariant manifolds are also represented. The state U^* in **Fig.** 4.4 corresponds to the secondary bifurcation point of the contact Hugoniot branches.

5. The Entropy and the Compatibility Conditions

In the construction of the Riemann solution, an *entropy criterion* is essential to select physically relevant solutions and to avoid multiplicity. By an *admissible* shock we mean a shock wave satisfying the entropy criterion in usage.

For the subsystem (4.1) in each plane $c = c_0$, the *viscous profile entropy criterion*, introduced by Courant and Friedrichs [1] and Gel'fand [2], is used with identity viscosity matrix. For contact discontinuities we use the following entropy condition, introduced in [4, 10]:

The contact entropy criterion: A state U_+ on a contact branch of $H(U_-)$ gives rise to an admissible discontinuity in the Riemann solution if:

a) U_+ lies on the local branch of $H(U_-)$ and the contact curve joining U_- to U_+ does not cross any coincidence surface, or

b) U_+ lies on a detached branch of $H(U_-)$ and there are states U_s and U_s', with U_s in the local branch of $H(U_-)$ and U_s' in the detached branch of $H(U_-)$, such that:

   i) the state U_s belongs to a coincidence surface;

   ii) the shock wave joining U_s to U_s' is admissible for the system (4.3) in the horizontal plane $c = c_s$ (i.e., it satisfies the viscous profile entropy criterion);

   iii) the contact curve joining U_s' to U_+ does not cross any coincidence surface.

In the context of flow in porous media this contact entropy condition means that the concentration of a substance injected in the phase with saturation u must vary monotonically in state space along an integral curve of the linearly degenerate field, [4]. In **Figs.** 6.3-6.7 in next section, the set of states on $H(U_-)$ that can be connected to U_- by an admissible contact discontinuity is represented by **thick** lines. We will use the nomenclature *admissible segments* to refer to connected portions of this set.

The states U_s and U_s' in the entropy criterion are such that the shock speed $\sigma(U_-;U_+)$ coincides with $\lambda^c(U_-) = \lambda^c(U_s) = \lambda^c(U_s') = \lambda^c(U_+)$. This means that in (x,t) space, there is no embedded sector of constant states between U_s and U_s'. Only one discontinuity is expressed separating U_- from U_+ in physical space, rather than three waves as suggested in state space.

Another fundamental restriction used to construct wave curves for Riemann solutions is the *geometric compatibility condition* between wave speeds. This condition reflects the fact that wave speeds in Riemann solutions increase in physical space (x,t) from U_L to U_R. This restriction forces portions of wave curves to be excized when elementary waves are concatenated to solve a Riemann problem.

6. Bifurcation Diagram for the Contact Curves

Let $U_0 = (u_0, v_0, c_0)$ be a state on the curve of singularities α. Assume that c_a and c_b are respectively the minimum and the maximum values for c in the three dimensional neighborhood $\mathcal{N}$ of U_0, where the Riemann problem will be considered. Without loss of generality, we assume that a contact curve through a state U_- in $\mathcal{N}$ either crosses the coincidence surface T^s or else extends from the level c_a to c_b into $\mathcal{N}$.

For each value of c in $[c_a, c_b]$, the equations (4.1) represent a strictly hyperbolic system of two conservation laws in a planar section $\mathcal{N}_c$ of $\mathcal{N}$, [9]. This system fails to be genuinely nonlinear along a straight line, where $\nabla\lambda^s \cdot e^s = 0$. According to §3, this line is the *slow inflection locus*. This straight line lies exactly on the plane π_1, which is one of the invariant manifolds of $\alpha(c)$. We remark that the existence of an inflection locus is precluded in the hypothesis of [5]. On the other hand, the peculiarity that the inflection locus consists of straight lines, all contained in a plane, does not affect the features of the solution we want to emphasize.

Because the characteristic directions associated to λ^s and λ^f are distinct, utilizing a change of variables, according to [7] one can see that the Riemann

problem for system (4.1) for each fixed c has a unique solution, defined by two wave groups. This means that the slow wave curves and the fast wave curves form a coordinate system for $\mathcal{N}_c$. In such a coordinate system, the solution of the Riemann problem with initial data $\{U_L; U_R\}$ in $\mathcal{N}_c$ is obtained by considering the backward wave curve through U_R and the forward wave curve through U_L. The intersection point between these two wave curves defines an intermediate constant state U_m, which separates the slow wave group from the fast wave group in the Riemann solution. The global construction of the Riemann solution for system (4.1) can be found in [9].

The neighborhood $\mathcal{N}$ is subdivided in eight regions by the surfaces T^s, π_1, S_1 and S_2. Here S_2 is the surface generated by slow integral curves through U_α as U_α varies on α. The subregions are L_1, L_2, L_3, L_4, and L_1', L_2', L_3', L_4', which are symmetric with respect to the plane π_1. In **Fig.** 6.1a we show a planar section of the global subdivision of state space Ω. In **Fig.** 6.1b we magnify $\mathcal{N}_c$ restricted to a plane of constant c. For simplicity we represent this restriction as a square. Due to the symmetry, left states for the Riemann solution will be considered only in L_1, L_2, L_3 and L_4. Actually the surface S_2 is not a boundary for the bifurcation diagram of contact curves. As we will see in §7, S_2 is a boundary separating left states U_L to be considered in the construction of the Riemann solution. On the other hand, the surface S_1 is a boundary for the bifurcation diagram of contact curves, but it is not a boundary for left states U_L in the construction of the Riemann solution.

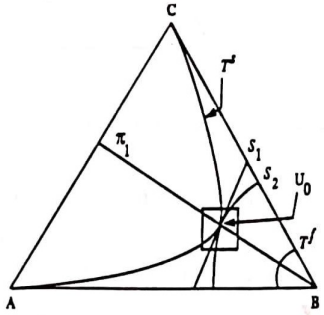

Fig. 6.1a: A planar section of the global subdivision of Ω.

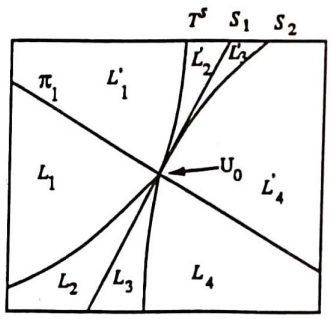

Fig. 6.1b: A magnified planar neigh-borhood of $U_0 \in \alpha(c)$.

In the figures throughout this work we use the following convention: dashed curves represent shock segments; curves with arrows represent rarefaction segments and crossed lines represent composite segments in the wave curves lying on horizontal planes $c = constant$.

In **Fig.** 6.2 typical (forward) slow wave curves for system (4.1) obtained in [9] are shown in $\mathcal{N}_c$ for a fixed value of $c \in [c_a, c_b]$. It is interesting to notice that for U_L in $L_1 \cup L_2 \cup L_3$, the slow wave curve based on U_L intersect the coincidence surface T^s, but for U_L in L_4 such intersection does not occur. The surface S_2 separates the states U_L possessing these two distinct behaviors.

Before describing the contact Hugoniot branches, we establish the labels and conventions used from **Fig.** 6.3 to **Fig.** 7.2b. First of all, each figure is a two-dimensional representation of the three-dimensional neighborhood $\mathcal{N}$. As we know from **Proposition 4.1**, the Hugoniot curve $H(U_-)$ for any state U_- consists of a part lying on the plane $c = c_-$ and of contact branches transversal to this plane. The projection of the contact branches onto the plane $c = c_-$ is indicated by a "3D" label.

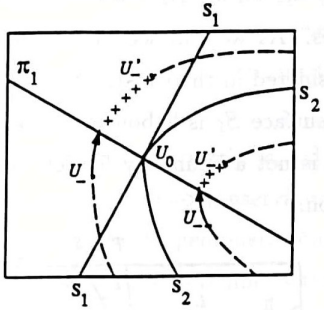

Fig. 6.2: Typical slow wave curves for the system (4.2).

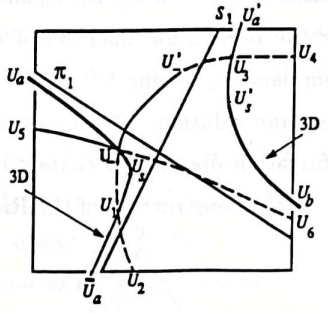

Fig. 6.3: Projection of $H(U_-)$ onto the plane $c = c_-$, for U_- in L_1.

In **Fig.** 6.3–6.7, the Hugoniot curves based on U_-, with $U_- \in \mathcal{N}$, are represented as follows. The states labeled by U_-, U'_-, $U_1, \cdots U_6$, lie on the plane $c = c_-$. The state U'_- corresponds to $\sigma(U_-; U'_-) = \lambda^s(U_-)$. The states U_-, U_1, U_3 are intersection points between contact branches and planar Hugoniot branches. They satisfy $\sigma(U_-; U_1) = \sigma(U_-; U_3) = \lambda^c(U_-) = \lambda^c(U_1) = \lambda^c(U_3)$.

The states labeled by U_a, $\bar{U}_a$ and U'_a lie on the plane $c = c_a$. The states labeled by U_b lie on the plane $c = c_b$. The states labeled by U_s lie on the plane $c = c_s \geq c_-$; they are defined by the intersection of $H(U_-)$ with the coincidence surface T^s. The states labeled by U'_s also lie on the plane $c = c_s$; according our contact entropy criterion the states U'_s correspond to initial points of detached admissible contact segments of the Hugoniot curves.

In **Figs.** 6.3–6.7, the Hugoniot branches lying on the plane $c = c_-$ are $[U_2U_-U'_-U_4]$ and $[U_5U_-U_6]$. Each state U_+ in the segment $[U_-U_2]$ or in the segment $[U'_-U_4]$ can be connected to U_- by an admissible slow shock. Each state U_+ in the segment $[U_-U_6]$ can be connected to U_- by an admissible fast shock.

Now let us describe the qualitative behavior of the contact Hugoniot branches. We have to consider five cases according to the localization of U_- in the subdivision of $\mathcal{N}$ in **Fig.** 6.1b.

Case 1. $U_- \in L_1$.

For U_- lying in L_1, **Fig.** 6.3, the projection of the contact Hugoniot branches on plane $c = c_-$ are the local segment $[U_aU_-U_sU_1\bar{U}_a]$ and the detached segment $[U'_aU_3U'_sU_b]$. Along the local contact branch in the three dimensional space, the value of c increases from c_a to c_s ($U_s \in T^s$) and decreases from c_s to c_a. Along the detached contact branch, c increases from the minimum value $c_a = c'_a$ to the maximum value c_b. According to our contact entropy criterion, the states U_+ in the local segment $[U_aU_-U_s]$ within L_1 and the states U_+ in the detached segment $[U'_sU_b]$ within $L'_3 \cup L'_4$ can be connected to U_- by an admissible contact discontinuity. We remark that the state U'_- in **Fig.** 6.3 may lie on either side of the surface S_1. The important thing is that U'_- belongs to the left hand side of state U_3 along the segment $[U_-U'_-U_3U_4]$.

Case 2. $U_- \in T^s$, the boundary between L_1 and L_2.

For U_- lying on the coincidence surface T^s, boundary between regions L_1 and L_2, the Hugoniot curve is represented in **Fig.** 6.4. In this case, the states

U_-, U_1 and U_s in the local contact branch coincide, as well as the states U'_-, U_3 and U'_s in the detached contact branch. According to our contact entropy criterion, the admissible contact segments are the local segment $[U_a U_- \bar{U}_a]$ and the detached segment $[U'_s U_b]$.

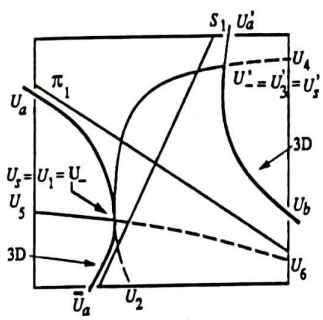

Fig. 6.4: Projection of $H(U_-)$ onto the plane $c = c_-$, for U_- on T^s.

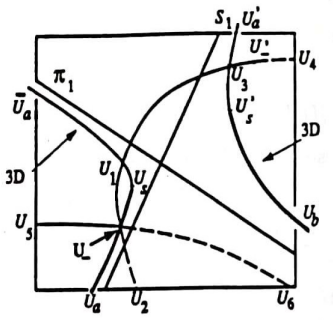

Fig. 6.5: Projection of $H(U_-)$ onto the plane $c = c_-$, for U_- in L_2.

Case 3. $U_- \in L_2$.

If U_- is moved from L_1 across T^s to L_2, the contact branches and the admissible segments are similar to the case when $U_- \in L_1$, but the states U_a and U_- in the local contact branch exchange position with $\bar{U}_a$ and U_1, respectively, relative to the Case 1 above. The admissible contact segments are $[U_a U_- U_s]$ and $[U'_s U_b]$.

Case 4. $U_- \in S_1$, the boundary between L_2 and $L_3 \cup L_4$.

For $U_- \in S_1$, **Fig.** 6.6, the contact branches suffer a nontrivial bifurcation. The states U_s and U'_s on the contact Hugoniot branches of the previous cases move towards each other and they meet at the secondary bifurcation point U_s^* on α in **Fig.** 6.6. This secondary bifurcation is illustrated also in **Fig.** 4.4 in three-dimensional state space (with $U_s^* = U^*$). In this case, the admissible contact segments correspond to the local segment $[U_a U_- U_s^*]$ on S_1, together

with the segment $[U_s^* U_b^*]$ on the invariant plane π_1.

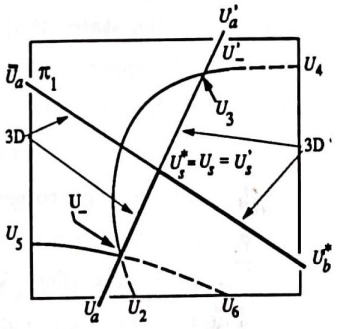

Fig. 6.6: Projection of $H(U_-)$ onto the plane $c = c_-$, for U_- on S_1.

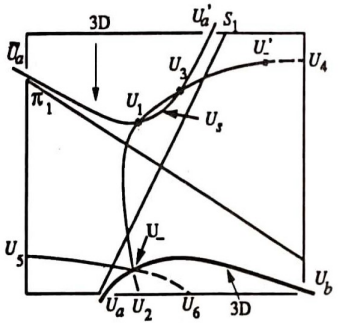

Fig. 6.7: Projection of $H(U_-)$ onto the plane $c = c_-$, for U_- in $L_3 \cup L_4$.

Case 5. $U_- \in L_3 \cup L_4$.

For U_- lying in $L_3 \cup L_4$, **Fig.** 6.7, the contact Hugoniot branches consist of the local branch $[U_a U_- U_b]$ together with the detached branch $[U_a' U_3 U_s U_1 \bar{U}_a]$. Comparing with the previous figures, notice that the states U_1 and U_s in **Fig.** 6.7 migrated to the detached contact branches, while the state U_b migrated from the detached to the local contact branch. In addition, the state U_s' of the previous figures disappeared. As opposed to the previous cases, here the local branch does not intersect any coincidence surface in the neighborhood of α, and the variable c varies monotonically from c_a to c_b. Thus, according to our entropy criterion, states on the local contact branch can be connected to U_- by admissible contact discontinuities, but states on the detached branch cannot.

Remark: If the projections of the contact branches of **Fig.** 6.5, **Fig.** 6.6 and **Fig.** 6.7 are drawn in a single picture, one can also identify the saddle behavior of the contact curves near α.

7.The Riemann Solution near $\alpha(c)$

For any given left state U_- outside the coincidence surface T^s, we have three distinct directions to follow when constructing wave curves through U_- in the three-dimensional state space Ω. The *lower wave curve*, denoted by $W^1(U_-)$,

consists of the states that can be connected to U_- by waves with lower speed. The *middle wave curve*, denoted by $W^2(U_-)$, consists of the states that can be connected to U_- by waves with intermediate speed. The *upper wave curve*, denoted by $W^3(U_-)$, consists of the states that can be connected to U_- by waves with upper speed.

We can choose the neighborhood $\mathcal{N}$ of $U_0 \in \alpha(c)$ small enough to ensure that $\lambda^s < \lambda^f$ and $\lambda^c < \lambda^f$. This means that the upper wave curves in $\mathcal{N}$ always coincide with the fast wave curve through U_- in horizontal slices $\mathcal{N}_c$ of $\mathcal{N}$. But, as we may have $\lambda^c = \lambda^s$, the lower and the middle wave curves consist of segments of either slow or contact waves. Since in $\mathcal{N}_c$ the system (4.1) is strictly hyperbolic for each fixed c, the fast (upper) wave curves are not tangent to the slow wave curves. The same argument is valid for the contact curves and the fast (upper) wave curves. Thus the upper wave curves for system (4.1) are tangent neither to the lower nor to the middle wave curves.

As we will see, although the wave curves for our model are only continuous and may possess jumps in derivatives at isolated states, a generalized Lax construction still works to obtain unique Riemann solutions.

In order to describe the Riemann solution we begin by building the forward lower wave $W^1(U_L)$. Then we construct a surface, which will be denoted by M, generated by middle wave curves based on states U_m, with U_m varying along $W^1(U_m)$. Finally, we are able to construct the Riemann solution for a given state U_R in Ω, using arguments based on transversality of the wave curves.

Remark: As we will see in the next, the Riemann problem for initial states restricted to the surface M consists of a straightforward generalization of the Riemann problem for the Keyfitz-Kranzer-Isaacson-Temple class of models for two conservation laws, [6, 4].

In the following, we will construct the surface M for generic initial left state U_L in $\mathcal{N}$. The surface M consists of portions of two types. Portions of the first type correspond to U_m varying along each segment of $W^1(U_L)$. Portions of the second type correspond to distinct segments of $W^2(U_m)$ for U_m varying in a

particular segment of $W^1(U_L)$.

We have to consider three distinct regions for U_L.

Case 1. $U_L \in L_1$.

This region is characterized by the inequalities $\lambda^c(U_L) < \lambda^s(U_L) < \lambda^f(U_L)$.

The Hugoniot curve through U_L (**Fig.** 6.3 with $U_L = U_-$) has the admissible contact segments $[U_aU_s]$, $[U_s'U_b]$. It also has two distinct slow shock segments $[U_LU_2]$ and $[U_L'U_4]$ on the plane $c = c_L$. Since $\lambda^c(U_L) < \lambda^s(U_L)$, the lower wave curve $W^1(U_L)$ starts at U_L by the admissible contact segment $[U_aU_s]$ (see **Fig.** 7.1a). The contact segment $[U_s'U_b]$ of **Fig.** 6.3 lies in $L_3' \cup L_4'$. It does not belong to $W^1(U_L)$ because contact discontinuities in this segment have speed values between $\lambda^s(U_L)$ and $\lambda^f(U_L)$. On the slow shock segments we have $\sigma(U_L; U_1) = \sigma(U_L; U_3) = \lambda^c(U_L)$. Since σ decreases from U_L to U_2 and from U_L' to U_4, we have that $\sigma(U_-; U) \leq \lambda^c(U_L)$ for all states U in the segments $[U_1U_2]$ and $[U_3U_4]$. Therefore the slow shock segments $[U_1U_2]$ and $[U_3U_4]$ also belong to $W^1(U_L)$. Thus, the lower wave curve $W^1(U_L)$ consists of the contact segment $[U_aU_s]$ and the slow shock segments $[U_1U_2]$, $[U_3U_4]$, as shown in **Fig.** 7.1a. The intersection point of $[U_1U_2]$ with the invariant manifold S_1 is labeled as U_7.

Let us construct the part of the surface M generated by $W^2(U_m)$, with U_m varying along the lower wave curve $W^1(U_L)$. The construction can be followed using **Fig.** 7.1b. In this figure, thick lines represent boundaries of smooth portions of the surface M; thin lines represent contact segments; and slow wave curve segments are represented by means of the same convention used in **Fig.** 6.2. We recall that slow wave curves have constant c while contact curves are transversal to planes with constant c.

The portion M_1 of M in **Fig.** 7.1b is generated by slow wave curve segments of $W^2(U_m)$ with U_m varying along the contact segment $[U_aU_s]$ of **Fig.** 7.1a. Due to the geometric compatibility condition, one end point of $W^2(U_m)$ lies on the contact segment $[\bar{U}_aU_s]$ while the other one lies on the detached contact segment $[U_a'U_s']$ of **Fig.** 7.1b (or **Fig.** 6.3). The boundaries of M_1 in **Fig.** 7.1b are the

contact segments $[\bar{U}_a U_1 U_s]$, $[U'_a U_3 U'_s]$ and the portion $[U_s U'_s]$ of $W^2(U_s)$.

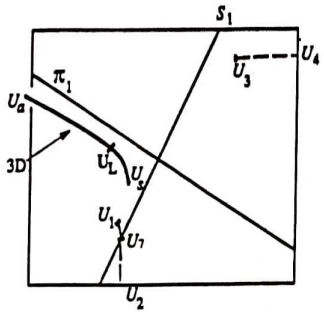

Fig. 7.1a: Projection of $W^1(U_L)$ for U_L in L_1.

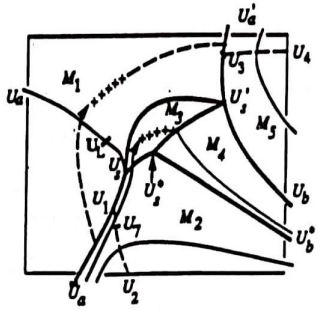

Fig. 7.1b: Projection of surface M for U_L in L_1.

Now let us consider the portions of the surface M generated by segments of $W^2(U_m)$, with U_m varying along $[U_1 U_2]$ of $W^1(U_L)$ in **Fig.** 7.1a. Since we have $\lambda^s(U_m) < \lambda^c(U_m) < \lambda^f(U_m)$ along $[U_1 U_2]$, the first segment of $W^2(U_m)$ must be the admissible contact segment through U_m. The surface M_2 in **Fig.** 7.1b is generated by such contact segments. Since U_7 lies on the invariant manifold S_1, $W^2(U_m)$ for $U_m \in [U_1 U_7) \subset L_2$ and for $U_m \in (U_7 U_2] \subset L_3$ have different behaviors. According to Case 5 in §6, as shown in **Fig.** 6.7 with $U_m = U_-$, the contact through U_m in $(U_7 U_2]$ does not intersect the coincidence surface T^s in a neighborhood of α; the segment extends from the plane $c = c_a$ to the plane $c = c_b$. If U_m belongs to $[U_1 U_7)$ (Case 3 in §6, **Fig.** 6.5 with $U_m = U_-$), the contact curve through U_m intersects the coincidence surface T^s at a state to be called U_β, (which corresponds to U_s in **Fig.** 6.5 and which is not drawn in **Fig.** 7.1b). In the limit case, when $U_m = U_7$, the contact curve through U_m has a secondary bifurcation exactly at the state U^*_s on the singular curve α (see **Fig.** 6.6 with $U_- = U_m$, or **Fig.** 4.4 with $U^*_s = U^*$). According to Case 4 in §6, the Hugoniot curve $H(U_7)$ has two admissible segments, one through U_7 (on the invariant manifold S_1) below U^*_s and another (on the invariant manifold π_1) up to state U^*_s. Recall that the curve α is the triple intersection of the surfaces T^s, S_1 and π_1. The surface M_2 in **Fig.** 7.1b shares the contact segment

$[\bar{U}_a U_s]$ (within L_2) as a boundary with the surface M_1. The segment $[U_s U_s^*]$ in **Fig.** 7.1b defined by the states U_β on T^s as well as the contact segment $[U_s^* U_b]$ of **Fig.** 6.6) are the other boundaries of M_2.

Since U_β lies on T^s, we have $\lambda^c(U_\beta) = \lambda^s(U_\beta)$. Thus $W^2(U_m)$ (for $U_m \in [U_1 U_7)$) can be continued at U_β by a slow rarefaction segment inwards L_1. According to the geometric compatibility condition, the end point of this segment of slow wave curve is a state U'_β, which lies in the detached contact branch of $H(U_m)$ (or of $H(U_\beta)$) in the plane $c = c_\beta \geq c_s$ (see **Fig.** 6.4 with $U_- = U_\beta$ and $U'_- = U'_\beta$). Notice that we have $\sigma(U_m; U'_\beta) = \lambda^c(U_m) = \lambda^c(U'_\beta) = \lambda^c(U_\beta) = \sigma(U_\beta; U'_\beta)$. The surface M_3 in **Fig.** 7.1b is generated by the slow wave curve segments through U_β that belong to $W^2(U_m)$, as U_m varies along $[U_1 U_7)$. The surface M_3 shares the segment $[U_s U_s^*]$ in **Fig.** 7.1b as a common boundary with M_2; it also shares the slow wave curve segment $[U_s U'_s]$ with M_1. The segment $[U'_s U_s^*]$ in **Fig.** 7.1b obtained as the locus of states U'_β when U_β varies on $[U_s U_s^*]$ is another boundary of M_3.

According to Case 3 in §6, the states along the contact segment up to U'_β are admissible to be connected to $U_m \in [U_1 U_7) \subset L_2$ (see **Fig.** 6.5 with $U_m = U_-$, $U_s = U_\beta$, and $U'_s = U'_\beta$). Since $\lambda^s(U'_\beta) < \lambda^c(U'_\beta) < \lambda^f(U'_\beta)$, this contact segment belongs to $W^2(U_m)$. The surface M_4 in **Fig.** 7.1b is generated by the admissible contact segments (of $H(U_m)$) through U'_β, as U_m varies along $[U_1 U_7)$. The surface M_4 shares the segment $[U'_s U_s^*]$ in **Fig.** 7.1b as a common boundary with M_3; it also shares the contact segment $[U_s^* U_b^*]$ (lying on π_1) as a common boundary with M_2. The contact segment $[U'_s U_b]$ in **Fig.** 7.1b is another boundary of M_4.

The portion M_5 is the last part of the surface M drawn in **Fig.** 7.1b. It is generated by the admissible contact segments based on U_m, which varies along the shock segment $[U_3 U_4]$ of $W^1(U_L)$ in **Fig.** 7.1a (see **Fig.** 6.7 with $U_m = U_-$ and use the symmetry). The surface M_5 shares the admissible contact segment $[U'_a U'_s]$ with surface M_1; it also shares the contact segment $[U'_s U_b]$ with surface M_4.

Now the surface M is complete. We have $M = M_1 \cup M_2 \cup M_3 \cup M_4 \cup M_5$, a

stratified surface. In order to construct the Riemann solution with initial data $\{U_L; U_R\} \in L_1 \times \mathcal{N}$, we start with the state U_R in $\mathcal{N}$ and first obtain the state U_m^2 as the intersection point of M with the backward upper (fast) wave curve through U_R. The state U_m^2 is well defined, because the surface M consists of slow and contact segments, which are transversal to upper wave curves. Next we define the state U_m^1 as the intersection point of the backward middle wave curve through U_m^2 with the forward lower wave curve through U_L. The state U_m^1 is well defined because M was generated by middle wave curves based on $W^1(U_L)$ with such wave curves transversal to $W^1(U_L)$. The Riemann solution possesses two intermediate constant states, U_m^1 and U_m^2, and consists of a lower wave group (which in turn consists of slow or contact waves) from U_L to U_m^1, followed by a middle wave group (which consists of slow and/or contact waves) connecting U_m^1 to U_m^2 and then an upper wave group (which consists of fast waves) connecting U_m^2 to U_R.

The structure of the Riemann solution of system (3.1) for U_L in subregion L_1 and U_R in $\mathcal{N}$ depends on the position of the state U_m^2 in M. If U_m^2 lies on M_1, the Riemann solution consists of the sequence contact/slow/fast wave groups; if U_m^2 lies on M_2, M_4 or M_5, it consists of a sequence slow/contact/fast wave groups; and if U_m^2 lies on M_3, the Riemann solution consists of a sequence slow/contact-slow/fast wave groups. We remark that if U_m^2 lies on M_4, the wave group contact-slow-contact used to connect U_m^1 to U_m^2 corresponds to a single contact discontinuity, with speed $\lambda^c(U_m^2) = \lambda^c(U_m^1)$. Finally, it is easy to verify that the solutions depend L^1_{loc}-continuously on U_L and U_R.

Case 2. $U_L \in L_2 \cup L_3$.

This region is characterized by the inequalities $\lambda^s(U_L) < \lambda^c(U_L) < \lambda^f(U_L)$ with the slow wave curve through U_L crossing the coincidence surface T^s.

The Hugoniot curve $H(U_L)$ for U_L in L_2 and for U_L in L_3 are drawn in **Fig.** 6.5 and **Fig.** 6.7 (with $U_L = U_-$), respectively. Since the construction of the surface M is similar in both cases, we will consider only $U_L \in L_3$. The lower wave curve $W^1(U_L)$ is shown in **Fig.** 7.2a. According to the inequalities above,

$W^1(U_L)$ starts at U_L as a slow wave curve (see **Fig.** 6.2). In one characteristic direction, the slow wave curve through U_L reaches the coincidence surface T^s at the state U_s, with $c_s = c_L$. In the opposite direction, there is no coincidence of wave speeds, and $W^1(U_L)$ reaches a boundary of $\mathcal{N}$ at the state U_2. The segment $[U_2U_s]$ crosses the invariant manifold S_1 at the state U_7. Since $\lambda^s(U_s) = \lambda^c(U_s)$, the lower wave curve $W^1(U_L)$ is continued into the region L_1 by the contact segment $[U_sU_a]$, with U_a lying on plane $c = c_a$ (see **Fig.** 6.4, with $U_- = U_s$). But the slow rarefaction segment $[U_LU_s]$ defines the composite segment $[U_s'U_L']$ with $U_L' \in L_3'$. The state U_L' in **Fig.** 7.2a corresponds to the state U_-' in **Fig.** 6.7. Since wave speeds along composite segments coincide with wave speeds of states along the corresponding rarefaction segment, we have that $[U_s'U_L']$ also belongs to $W^1(U_L)$. The slow wave curve is continued at U_L' by the shock segment $[U_L'U_4]$, which corresponds to the segment $[U_-'U_4]$ in **Fig.** 6.7. Since $\sigma(U_L; U_L') = \lambda^s(U_L) < \lambda^c(U_L) = \sigma(U_L; U_3)$ and σ decreases from U_L' to U_4, U_L can be connected to each state on segment $[U_L'U_4]$ by a *Lax 1-shock* of system (4.1). In other words, $[U_L'U_4]$ belongs to $W^1(U_L)$.

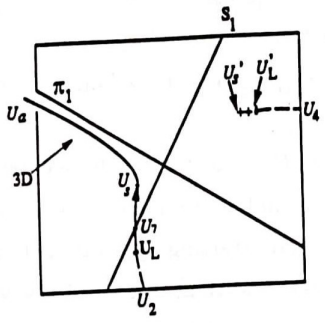

Fig. 7.2a: Projection of $W^1(U_L)$ for U_L in $L_2 \cup L_3$.

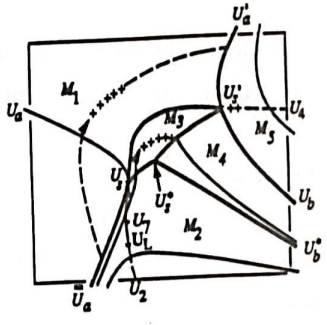

Fig. 7.2b: Projection of surface M for U_L in $L_2 \cup L_3$.

Let us to construct the surface M, generated by middle wave curves through U_m, with U_m varying along the lower wave curve $W^1(U_L)$ in **Fig.** 7.2a. The construction is shown in **Fig.** 7.2b. We begin the construction of M for U_m on the contact segment $[U_aU_s]$ of $W^1(U_L)$ in **Fig.** 7.2a. Since $[U_aU_s]$ lies within

region L_1, $W^2(U_m)$ must start by a slow wave curve segment. According to the geometric compatibility condition, one end point of $W^2(U_m)$ is a state on the local contact segment $[\bar{U}_a U_s]$ of **Fig.** 7.2b (or **Fig.** 6.4); the other end point of $W^2(U_m)$ lies on the nonlocal contact segment $[U'_a U'_s]$ of the same **Fig.** 7.2b (or **Fig.** 6.4). The portion M_1 of M in **Fig.** 7.2b is generated by slow wave curve segments of $W^2(U_m)$, as U_m varies on the contact segment $[U_a U_s]$ of $W^1(U_L)$. The boundaries of surface M_1 are the contact segment $[\bar{U}_a U_s]$ (within region L_2), the slow wave curve segment $[U_s U'_s]$, and the contact segment $[U'_a U'_a]$.

Now let U_m be a state on the segment $[U_s U_2]$ of $W^1(U_L)$ in **Fig.** 7.2a. For $U_m \in [U_s U_7)$, the shape of $H(U_m)$ is the same as that of $H(U_-)$ in **Fig.** 6.5, and for $U_m \in (U_7 U_2]$ the shape of $H(U_m)$ is the same as that of $H(U_-)$ in **Fig.** 6.7. Since $\lambda^s(U_m) < \lambda^c(U_m)$, the middle wave curve $W^2(U_m)$ starts as a contact segment through U_m. The portion M_2 of M, represented in **Fig.** 7.2b, is generated by such admissible contact segments, as U_m varies along $[U_s U_2]$ of **Fig.** 7.2a. The contact segment $[\bar{U}_a U_s]$ in **Fig.** 7.2b (which lies within L_2) is a common boundary with the surface M_1. This boundary is continued by the segment $[U_s U^*_s]$. The segment $[U_s U^*_s]$ is defined by the intersection of M_2 with the coincidence surface T^s. Again the state U^*_s is the secondary bifurcation point of $H(U_7)$. The contact segment $[U^*_s U^*_b]$ in **Fig.** 7.2b is also a boundary of M_2.

For U_m on the segment $[U_s U_7)$ in **Fig.** 7.2a, let U_β be a state in the segment $[U_s U^*_s]$ in **Fig.** 7.2b. Since $\lambda^c(U_\beta) = \lambda^s(U_\beta)$, the middle wave curve $W^2(U_m)$ can be continued at U_β into L_1 by a slow wave curve, starting by a rarefaction segment. According to the geometric compatibility condition, this middle wave curve stops at the state U'_β (U'_s in **Fig.** 6.4) such that $\lambda^s(U_\beta) = \sigma(U_\beta; U'_\beta) = \lambda^c(U_\beta) = \lambda^c(U'_\beta)$. The portion M_3 of M in **Fig.** 7.2b is generated by segments $[U_\beta U'_\beta]$ of $W^2(U_m)$, as U_m varies along the segment $[U_s U_7)$ of $W^1(U_L)$. The surface M_3 shares the segment $[U_s U^*_s]$ in **Fig.** 7.2b as common boundary with the surface M_2. The segment $[U^*_s U'_s]$ defined by the states U'_β, and the slow wave curve segment $[U_s U'_s]$ are other boundaries of M_3 in **Fig.** 7.2b.

Since we have $\sigma(U_\beta; U'_\beta) = \lambda^c(U'_\beta)$ and $\lambda^c(U'_\beta) > \lambda^s(U'_\beta)$, the middle wave

curve $W^2(U_m)$ (for $U_m \in [U_s U_7]$ in **Fig.** 7.2a) is continued by the portion of the admissible contact segment up to U'_β (see **Fig.** 6.5 with $U_m = U_-$, $U_s = U_\beta$ and $U'_s = U'_\beta$). According to Case 3 in §6, this contact segment of $H(U_m)$ satisfies the contact entropy condition. The portion M_4 of surface M in **Fig.** 7.2b consists of such admissible contact segments through U'_β, as U_m varies along $[U_s U_7]$. The surface M_4 shares the segment $[U^*_s U'_s]$ in **Fig.** 7.2b as a common boundary with the surface M_3; The surface also shares the contact segment $[U^*_s U^*_b]$ with the surface M_2. The contact segment $[U'_s U_b]$ is another boundary of M_4.

The portion M_5 of M in **Fig.** 7.2b is generated by the admissible contact segments through U_m varying along $[U'_s U_4]$ of $\mathcal{W}^1(U_L)$ in **Fig.** 7.2a. The surface M_5 shares the contact segment $[U'_a U'_s]$ as a common boundary with surface M_1, as well as $[U'_s U_b]$ as a common boundary with the surface M_4.

Thus the surface $M = M_2 \cup M_3 \cup M_4 \cup M_1 \cup M_5$ is now complete. The Riemann solution for an arbitrary state U_R in a neighborhood of $U_0 \in \alpha$ is obtained as in Case 1: we obtain the intermediate states $U^2_m \in M$ and $U^1_m \in W^1(U_L)$ by constructing the backward wave curves through U_R and U^2_m, respectively. If $U^2_m \in M_1$, the sequence consists of slow-contact/slow/fast wave groups. If $U^2_m \in M_2 \cup M_4 \cup M_5$, the Riemann solution consists of the sequence slow/contact/fast wave groups. Finally, if $U^2_m \in M_3$ the sequence consists of slow/contact-slow/fast wave groups.

Case 3. $U_L \in L_4$.

This region is characterized by the inequalities $\lambda^s(U_L) < \lambda^c(U_L) < \lambda^J(U_L)$; however, the slow wave through U_L does not cross the coincidence surface T^s. Thus the lower wave curve coincides with the slow wave curve on plane $c = c_L$. This implies that the portions M_1, M_3 and M_4 of the previous cases vanish. According to Case 5 of §6 (and using the symmetry), the middle wave curves $W(U_m)$, with U_m varying along $W^1(U_L)$, consist only of the (local) admissible contact segments of $H(U_m)$. Such contact segments extend from c_a to c_b (see **Fig.** 6.7 and use the symmetry). Thus the surface M consists of only one portion, generated in the same way as the portions M_2 and M_5 in the previous

cases, by admissible contact segments. The Riemann solution for an arbitrary right state U_R is simpler than the previous cases. The sequence of waves in the Riemann solution is always slow/contact/fast wave groups.

Acknowledgments. We thank the Departamento de Sistemas da Computação da Universidade Federal da Paraíba - Campus II, for the usage of its computational facilities.

References

[1] R. Courant, K. Friedrichs, *Supersonic flow and shock waves*, John Wiley & Sons, New York, (1948).

[2] I. M. Gel'fand, *Some problems in theory of quasi-linear equations*, Amer. Math. Soc. Trans., Ser. 2, 29 (1963), pp. 295–381.

[3] M. Golubitsky, D. G. Shaeffer, *Singularities and Groups in Bifurcation Theory*, vol. I, Springer Verlag, 1985.

[4] E. Isaacson, *Global solution of a Riemann problem for a non-strictly hyperbolic system of conservation laws arising in enhanced oil recovery*, preprint, Rockefeller University, New York, (1981).

[5] E. Isaacson, B. Temple, *Nonlinear Resonance in Systems of Conservation Laws*, SIAM J. Appl. Math., vol. 52, #5, (1992), 1260–1278.

[6] B. Keyfitz, H. Kranzer, *A system of non-strictly hyperbolic conservation laws arising in elasticity theory*, Arch. Rat. Mech. Anal., 72 (1980), 219–241.

[7] T. P. Liu, *The Riemann problem for a general systems of conservation laws*, J. Diff. Eq. 18 (1975), 218–234.

[8] J. Smoller, *Shock Waves and Reaction Diffusion Equations*, Springer Verlag, 1983.

[9] A. J. de Souza, *Stability of Singular Fundamental Solutions Under Perturbations for Flow in Porous Media*, Comp. and Appl. Math., vol. 11, #2, (1992), 73–115.

[10] A. J. de Souza, *Wave structure for a non-strictly hyperbolic system of three conservation laws*, Notas de Matemática *n.°* 01, DME/CCT/UFPB, (1993).

[11] B. Temple, *Systems of Conservation Laws with Invariant submanifolds*, Trans. Amer. Math. Soc., vol. 280, #2, (1980), 781–795.

Intituto de Matemática
Pura e Aplicada
Estrada Dona Castorina, 110
22460-320, Rio de Janeiro, RJ
Email: marchesi@fluid.impa.br

Universidade Federal da Paraíba,
Departamento de Matemática e
Estatística
58109-970, Campina Grande, PB, Brazil
Email: desouza@brufpb2.bitnet